

# Deep Unsupervised Key Frame Extraction for Efficient Video Classification

HAO TANG\*, ETH Zurich, Switzerland

LEI DING, University of Trento, Italy

SONGSONG WU, Guangdong University of Petrochemical Technology, China

BIN REN, University of Trento, Italy

NICU SEBE, University of Trento, Italy

PAOLO ROTA, University of Trento, Italy

Video processing and analysis have become an urgent task since a huge amount of videos (e.g., Youtube, Hulu) are uploaded online every day. The extraction of representative key frames from videos is very important in video processing and analysis since it greatly reduces computing resources and time. Although great progress has been made recently, large-scale video classification remains an open problem, as the existing methods have not well balanced the performance and efficiency simultaneously. To tackle this problem, this work presents an unsupervised method to retrieve the key frames, which combines Convolutional Neural Network (CNN) and Temporal Segment Density Peaks Clustering (TSDPC). The proposed TSDPC is a generic and powerful framework and it has two advantages compared with previous works, one is that it can calculate the number of key frames automatically. The other is that it can preserve the temporal information of the video. Thus it improves the efficiency of video classification. Furthermore, a Long Short-Term Memory network (LSTM) is added on the top of the CNN to further elevate the performance of classification. Moreover, a weight fusion strategy of different input networks is presented to boost the performance. By optimizing both video classification and key frame extraction simultaneously, we achieve better classification performance and higher efficiency. We evaluate our method on two popular datasets (i.e., HMDB51 and UCF101) and the experimental results consistently demonstrate that our strategy achieves competitive performance and efficiency compared with the state-of-the-art approaches.

Additional Key Words and Phrases: Key Frame Extraction; Density Peaks Clustering; LSTM; Weight Fusion; Unsupervised Learning; Video Classification

## ACM Reference Format:

Hao Tang, Lei Ding, Songsong Wu, Bin Ren, Nicu Sebe, and Paolo Rota. 2018. Deep Unsupervised Key Frame Extraction for Efficient Video Classification. In *Woodstock '18: ACM Symposium on Neural Gaze Detection, June 03–05, 2018, Woodstock, NY*. ACM, New York, NY, USA, 16 pages. <https://doi.org/10.1145/1122445.1122456>

## 1 INTRODUCTION

Recent years have witnessed an exponential growth in video data availability on the web, such as Youtube. In this situation, large-scale video classification techniques [3, 5, 10, 12–14, 18, 21, 24, 31, 32, 43, 54, 57, 67, 69–71, 74–76] have also received increasing interests due to the fact that there is an increasing demand for efficient indexing and managing of these video data.

---

Permission to make digital or hard copies of all or part of this work for personal or classroom use is granted without fee provided that copies are not made or distributed for profit or commercial advantage and that copies bear this notice and the full citation on the first page. Copyrights for components of this work owned by others than ACM must be honored. Abstracting with credit is permitted. To copy otherwise, or republish, to post on servers or to redistribute to lists, requires prior specific permission and/or a fee. Request permissions from permissions@acm.org.

© 2018 Association for Computing Machinery.

Manuscript submitted to ACM

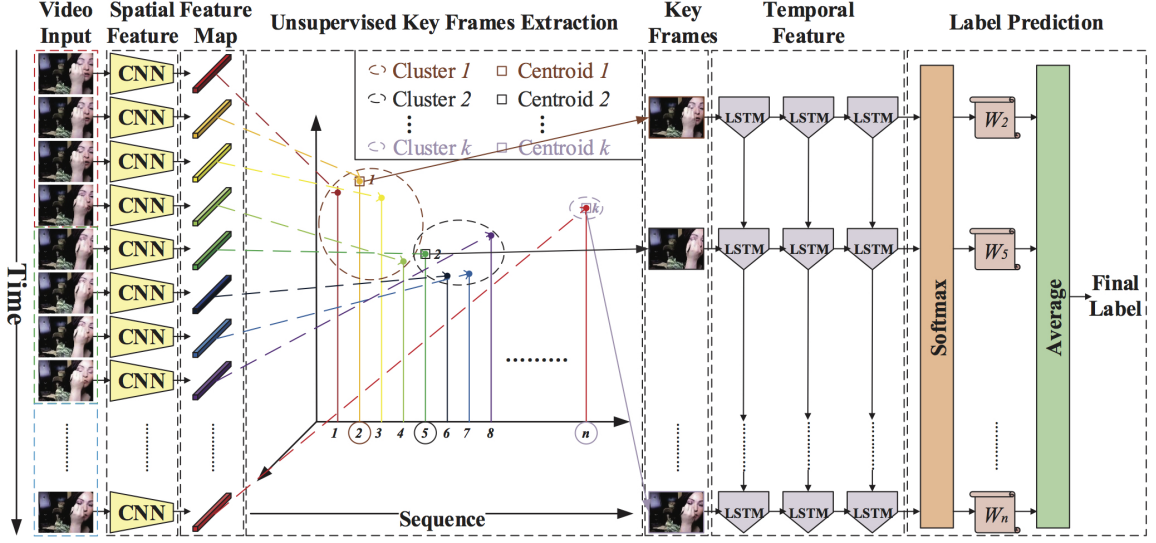


Fig. 1. The pipeline of the proposed large-scale video classification, which has three components, i.e., CNN, TSDPC and LSTM. The TSDPC is an unsupervised key frame extraction method which preserves the temporal information of the video and calculates the number of key frames automatically. The CNN-TSDPC is proposed for accelerating video processing. In addition, a LSTM cell is further connected at the end of the CNN, which is able to elevate the performance of video classification. At last, the LSTM predicts the video label at each key frame and we average these predictions for final labels.

Efficient and accurate large-scale video classification performance relies on the extraction of discriminative spatial and temporal features. Conventional approaches extract information or feature using hand-crafted features (e.g., Histogram of Optical Flow (HOF) [30] or improved Dense Trajectories (iDT) [63]) from video frames which are then encoded (e.g., Fisher Vector (FV) [63]) and pooled (e.g., average pooling) to produce a global feature representation and then passed to a classifier (e.g., SVM).

In recent years, video classification research has been influenced by the trends of deep learning. A common pipeline of these works is to use a group of frames as the input to the network, whereby the model is expected to learn spatio-temporal features. Simonyan et al. [48] propose a two-stream ConvNet architecture which incorporates spatial and temporal networks to extract spatial and temporal features. Feichtenhofer et al. [15] study a number of ways of fusing ConvNet towers both spatially and temporally in order to best take advantage of this spatio-temporal information. Wang et al. [67] present the Temporal Segment Network (TSN), which combines a sparse temporal sampling strategy and video-level supervision to enable efficient and effective learning using the whole action video. Ji et al. [23] introduce a 3D CNN model, in which both spatial and temporal features are extracted by performing 3D convolution. Tran et al. [55] propose an approach for spatio-temporal feature learning using deep 3-dimensional convolutional networks (3D ConvNets).

However, these approaches for video classification treat the videos in a holistic way, i.e., as one data instance. Feature representation learned from the entire video unavoidably brings redundant information from the repeated and unrelated video frames which leads to two problems, (i) one is that processing the whole video data requires excessive computational resources and time, for example, Kulhare et al. [28] report that the optical flow data on 13K videos was 1.5 TB. From the computational time perspective, these methods require extensively long periods of training time to

effectively optimize millions of parameters that represent the model; (ii) another problem is that repeated and unrelated video frames such as blurry, feature-less and background frames always overwhelm the targeted visual patterns, which sometimes confuse the classifier.

To fix these problems, many efforts have been done to explore the key frame extraction methods which can convert video processing to image processing. For example, Donahue et al. [9] employ a Long Short-Term Memory network (LSTM) which is connected to the output of the underlying CNN. However, this framework processes 16 sample frames selected evenly with a stride of 8 frames from the full length video as the video representation. Such average selection of samples may not consider all useful motion and spatial information. Besides, Zhu et al. [75] propose a key volume mining deep framework to identify key volumes to achieve high accuracy, but with a steep increase of the computational load.

To solve both limitations, we present a novel framework to model video representation in an efficient and accurate manner. Instead of trying to learn features over the entire video as in previous works, which always contain redundant information, resulting in degraded performance. We consider a different manner to extract video features over several key frames of the entire video, which is a fundamental way to alleviate the computation burden. Key frames, also named representative frames, are often employed to represent the story of a video. Key frame extraction is the key technology for video abstraction, which can remove the redundant information in the video and reduce the high computing redundancy between adjacent frames. The algorithm for key frame extraction will affect the reconstruction of video content.

To this end, we propose an unsupervised key frame extraction method by using Convolutional Neural Networks (CNNs) and Density Peaks Clustering (DPC) [44]. More specifically, we extract convolutional deep feature for each frame in the video and then map these deep feature maps into a high dimensional feature space. After that, how to describe the feature space is a hard nut to crack for its uneven distribution. To solve this, we propose the Temporal Segment Density Peaks Clustering (TSDPC) to select key frames in an unsupervised way in feature space. In order to preserve the temporal cues of the video, we first segment it into several segments, then select key frames on each segment using DPC. Finally, we combine all the key frames extracted from each segment to form the final key frames. TSDPC has two advantages compared with previous clustering-based method, (i) Previous clustering approaches cannot detect non-spherical clusters due to the fact that they only rely on the distance between feature points to do clustering. While TSDPC is the approach based on the local density of feature points, which is able to detect non-spherical clusters. (ii) Clumsy tricks are used to ensure the number of key frames which may bring uncertainty in previous works, while for TSDPC, it can calculate the number of key frames automatically.

After extracting key frames, we replace the original video sequence with the key frames as a surrogate for analyzing, which could greatly enhance the time efficiency with little cost of accuracy. In addition, in order to improve the accuracy, a Long Short-Term Network (LSTM) is further connected at the end of the CNN. Furthermore, a novel input network fusion strategy with different weights is presented. The pipeline of the proposed large-scale video classification framework is shown in Figure 1. Finally, experimental results show that the proposed framework is accurate and efficient for video classification on two public datasets.

The contributions of this work can be summarized as follows:

- We propose a novel method of unsupervised key frames extraction in video, CNN-TSDPC, which is comprised of CNN and Temporal Segment Density Peaks Clustering (TSDPC). Note that the proposed TSDPC can preserve the temporal information of a video and calculate the number of key frames automatically.

- The proposed CNN-TSDPC-LSTM framework is trained in an end-to-end fashion to improve both performance and efficiency for the video classification task.
- We present a weight fusion strategy of different input networks, in which different inputs are fused with different weights to elevate the accuracy of video classification.
- The proposed method and framework achieve competitive performance and are more efficient compared with the state-of-the-art models.

## 2 RELATED WORK

Video content summarization has been widely used to facilitate the indexing of large videos. In earlier works on video summarization, key frames are selected either by sampling video frames randomly or uniformly at certain time intervals. To make a key frame extraction algorithm effective, the extracted key frames should represent the whole video content without missing important information such as people and objects. While at the same time, video content information of these key frames should not be similar, in order to avoid content redundancy. In recent years, many algorithms have been proposed for key frame extraction in videos. There are three categories of key frames extraction algorithms.

**Segmentation Based.** These methods detect abrupt changes in terms of similarity between successive frames. The key frames are equidistant in the video curve with respect to Iso-Content Distance, Iso-Content Error and Iso-Content Distortion in [39]. In [11], a key frame is extracted if and only if the inter-frame difference overtakes a certain threshold. A key frame selection method based on key points is presented in [20], in which a global pool of key points based on SIFT feature extracted from all frames is generated and those frames that best cover the global key point pool are selected as key frames. In a word, this type of key frame extraction methods have the disadvantage, i.e., it may extract similar key frames if the same content reappears during a video.

**Dictionary Based.** These types of approaches convert key frames extraction into a sparse dictionary selection problem. In [6], a key frame selection method is proposed which is based on the sparse dictionary selection with the loss in  $L_{2,1}$  norm. Besides, the key frames are selected based on the true sparse constraint  $L_0$  norm to represent the whole video in [36].  $L_{2,0}$  constrained sparse dictionary selection model is proposed to solve the problems that the solution based on the convex relaxation cannot guarantee the sparsity of the dictionary and it selects key frames in a local point of view in [35]. In [37], a video is summarized into a few key objects by selecting representative object proposals generated from video frames based on the sparse dictionary selection method. To find key frames with both diversity and representativeness, the objective function in [61] consists of a reconstruction error and three structured regularizers, i.e., group sparsity regularizer, diversity regularizer, and locality-sensitivity regularizer.

**Clustering Based.** These approaches cluster frames into groups and then select the frames closest to the cluster centers as key frame. In [77], key frames are detected using unsupervised clustering based on visual variations. While in [26], dynamic delaunay clustering is adopted to extract key frames. Key frames are selected based on color feature using the k-means clustering algorithm in [7]. In [59], spectral clustering on spatio-temporal features is employed to extract key frames. Moreover, the mutual information values of these consecutive frames are clustered into several groups using a split-merge method in [4]. In [40], the problem is modeled as a graph clustering problem and it is solved using a skeleton graph. Besides, the authors present a key frame extraction approach based on local description and graph modularity clustering in [19].

However, the proposed CNN-TSDPC framework has three advantages compared with these approaches, (i) our framework can capture the discriminative spatial information by using a sophisticated CNN feature extractor. (ii) our

framework can represent the temporal information by using a temporal segmentation strategy. (iii) our framework can extract more representative key frames with less redundant information than previous works.

### 3 METHOD

We assume that a video  $\mathbf{V}$  can be divided into  $K$  segments  $\{V_1, V_2, \dots, V_K\}$  of equal durations. For each segment  $V_K$ , we assume that a frame in  $V_K$  can be represented by  $\mathbf{f}_i^K$ , where  $i \in [1, 2, \dots, N]$  and  $N$  is the number of frames in  $V_K$ ,

$$V_K = \{\mathbf{f}_i^K\}_{i=1}^N. \quad (1)$$

Hence, the key frame set  $\mathbf{f}_{m_k}^K$  is defined as follows:

$$\mathbf{f}_{m_k}^K = \Theta(V_K), k \in [1, 2, \dots, n_c], \quad (2)$$

where  $m_k$  is the index of the key frames,  $n_c \geq 1$  is the number of key frames and  $\Theta$  denotes the key frames extraction procedure, the objective is to remove the redundant data which will significantly reduce the amount of information to be processed. It is necessary to discard the frames with repetitive or redundant information during the extraction. Thus, key frame extraction is the fundamental step in video analysis applications.

#### 3.1 Convolutional Deep Feature Extraction

We try to find a proper descriptive index to evaluate each frame in a segment  $V_K$ , facilitating key frame extraction. Informative frames could better summarize the whole video, but how to quantify the information each frame contains is a hard nut to crack. Previous works such as [7] adopt the color feature to represent each frame. [54] uses the image entropy as a feature representation for hand action recognition. However, we argue that these feature extractors are not powerful to extract discriminative information. In this paper, we use CNNs to extract the deep feature. CNNs are powerful due to their ability to extract the semantic features of an image. The first few convolutional layers can identify lines and corners, and then we pass these patterns down through more convolutional layers and start recognizing more complex and abstract semantic features as we go deeper. This property makes CNNs really good at extracting features in images and videos.

For each frame  $\mathbf{f}_i^K$  in the segment  $V_K$ , we adopt ResNet [22] as deep feature extractor. This pre-trained model of ResNet is trained on a subset of the ImageNet dataset [45]. The model is trained on more than one million images and can classify images into 1,000 object categories. The feature vector  $\mathbf{x}_i^K$  can be obtained as follows:

$$\mathbf{x}_i^K = \Delta(\mathbf{f}_i^K), i \in [1, 2, \dots, N] \quad (3)$$

where  $\Delta$  denotes CNN feature extraction operation and  $\mathbf{x}_i^K$  is the corresponding feature vector of frame  $\mathbf{f}_i^K$ . After extracting deep features of each frame via feature extractor, feature vectors  $\mathbf{x}_i^K, i \in [1, 2, \dots, N]$  are then mapped to the points in high dimension feature space  $\mathcal{F}$ .

#### 3.2 Temporal Segment Density Peaks Clustering

We define the following symbols for the sake of simplicity,

$$S = \{\mathbf{x}_i^K\}_{i=1}^N, I_S = \{1, 2, \dots, N\}. \quad (4)$$

We consider that the distribution of  $S$  in  $\mathcal{F}$  should have the following two characteristics: (i) the cluster centers of  $S$  are surrounded by neighbors with a lower local density; (ii) these centers have a relatively large distance from any points

with a higher local density. Thus, we adopt density peaks clustering to further cluster these feature vector  $\mathbf{x}_i^K$ . Density peaks clustering [44] could better catch the delicate spherical structure of space where points reside than traditional clustering strategies, e.g., K-means, in which features are grouped to the nearest cluster center.

For each point  $\mathbf{x}_i^K$  in  $S$ , we compute two quantities: the local density  $\rho_i$  and its distance  $\delta_i$  from points of higher density. Both of these quantities depend only on the distance  $d_{ij}$  between points in  $\mathcal{F}$ ,

$$d_{ij} = \text{dist}(\mathbf{x}_i^K, \mathbf{x}_j^K) \quad (5)$$

The local density  $\rho_i$  of point  $\mathbf{x}_i$  is defined as:

$$\rho_i = \sum_{j \in \{I_S - \{i\}\}} \chi(d_{ij} - d_c), \quad (6)$$

where,

$$\chi(x) = \begin{cases} 1, & x < 0; \\ 0, & x \geq 0, \end{cases} \quad (7)$$

and  $d_c$  is a cutoff distance. Basically,  $\rho_i$  equals to the number of points that are closer than  $d_c$  to point  $\mathbf{x}_i^K$ . The algorithm is sensitive only to the relative magnitude of  $\rho_i$  in different points, which implies that, the results of the analysis are robust with respect to the choice of  $d_c$  for large dataset. A different way to define  $\rho_i$  is:

$$\rho_i = \sum_{j \in \{I_S - \{i\}\}} e^{-(\frac{d_{ij}}{d_c})^2}, \quad (8)$$

in which a Gaussian kernel is used to calculate the local density. We can see from these two definitions that the cutoff kernel in Eq. (6) is a discrete value, while Gaussian kernel in Eq. (8) is a continuous value, which guarantees a smaller probability of conflict. In other words, the probability that different point have the same local densities,  $\rho_i$ , is smaller.

Another important quantity is  $\delta_i$ , which is measured by the minimum distance between the point  $\mathbf{x}_i^K$  and any other point with higher density:

$$\delta_i = \begin{cases} \min_{j \in I_S^i} \{d_{ij}\}, & I_S^i \neq \emptyset; \\ \max_{j \in I_S} \{d_{ij}\}, & I_S^i = \emptyset, \end{cases} \quad (9)$$

where,

$$I_S^i = \{k \in I_S : \rho_k > \rho_i\}. \quad (10)$$

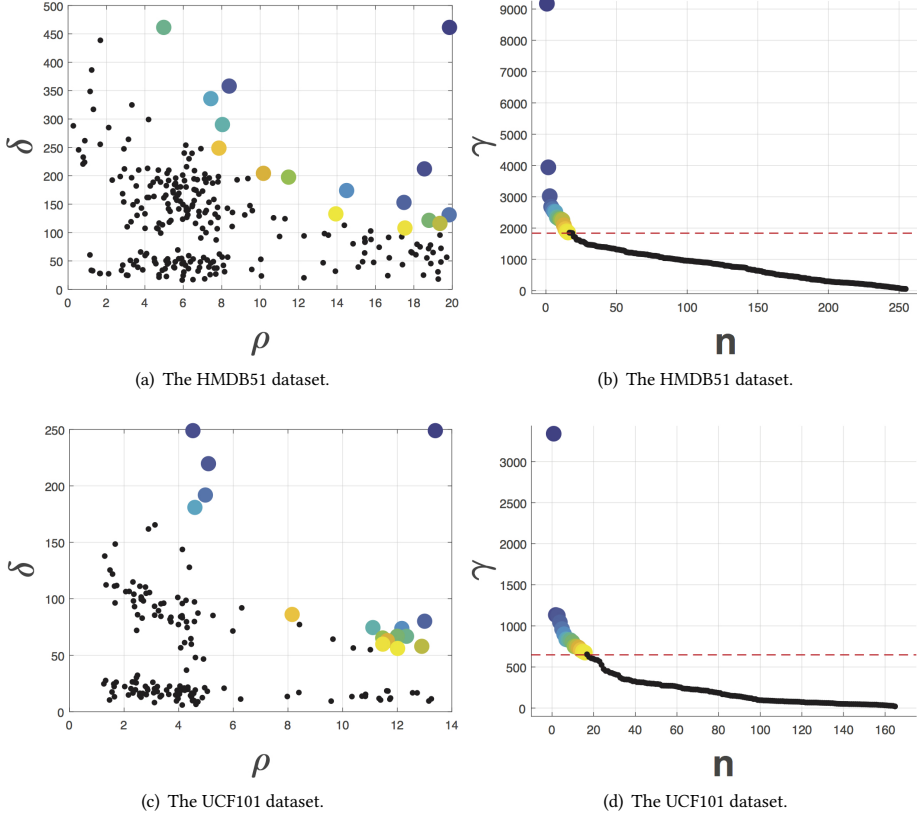
Obviously, the  $I_S^i = \emptyset$  if  $\rho_i = \max_{j \in I_S} \rho_j$ .

Consequently, for each point  $\mathbf{x}_i^K$  in the  $S$ , we can calculate binary pair  $(\rho_i, \delta_i)$ , where  $i \in I_S$ . The definition of quantity  $\gamma_i$  which considers both  $\rho_i$  and  $\delta_i$  is as follows,

$$\gamma_i = \rho_i \delta_i, i \in I_S, \quad (11)$$

we select the point with the larger value of  $\gamma_i$  as the cluster center. Figure 2 shows the selection of  $\rho$ ,  $\delta$  and  $\gamma_i$  on two videos of HMDB51 and UCF101 datasets, respectively.

In experiments, according to previous works on temporal modeling [17, 64, 67] we set  $K$  to 3. Since we observe that when  $K = 1$ , the key frames extracted by the proposed method cannot preserve the temporal information in the whole input video. We do the same operations on other segments and combine all the key frames from each segment to form the final key frames  $\mathbf{f} = \{\mathbf{f}^1, \mathbf{f}^2, \dots, \mathbf{f}^K\}$  of the video  $\mathbf{V}$ .

Fig. 2.  $\rho$ ,  $\delta$  and  $\gamma_i$  on HMDB51 and UCF101 datasets, respectively.

The pipeline of the proposed CNN-TSDPC framework is summarized in Algorithm 1. The CNN-TSDPC method is comprised of three steps. The first step is to segment a video into several volumes equally (step 1.1). The second step is convolutional deep feature extraction, we extract deep feature vector  $\mathbf{x}_i$  using Eq. (3) and then map feature vector  $\mathbf{x}_i$  to feature space  $\mathcal{F}$  (step 2.1 and step 2.2). After that, we conduct density peaks clustering operation. We first calculate the distance  $d_{ij}$  between  $\mathbf{x}_i$  and  $\mathbf{x}_j$ , and then calculate the cut off distance  $d_c$  with the given  $t$  (step 3.1 and step 3.2). According to the asseverations in [44],  $d_c$  can be selected as the rule that the average number of neighbors is around 1% to 2% of the total number of points in the data set. In order to obtain  $\gamma_i$ , we need to calculate  $\rho$  and  $\delta$  with Eq. (6) or Eq. (8) and Eq. (9) (step 3.3 and step 3.4). And then multiply  $\rho$  and  $\delta$  to obtain  $\gamma$  using Eq. (11) (step 3.5). Next, we rank  $\gamma_i$  in descending order and choose the  $n_c$  largest  $\gamma$  values as the clustering centers. In the end of our algorithm, the index of the key frames  $m_k$  and key frames  $\{\mathbf{f}_{m_k}\}_{k=1}^{n_c}$  of  $V_K$  are returned for further processing.

#### 4 LARGE-SCALE VIDEO CLASSIFICATION

To perform the sequential image classification, we employ Long Short-Term Memory networks (LSTMs), which is added at the top of CNNs. LSTMs have been widely used to advance the state-of-the-art of many difficult problems because they are effective at capturing long term temporal dependencies. We adopt the LSTM unit in our large-scale video classification

---

**Algorithm 1** The pipeline of the proposed CNN-TSDPC method.

---

**Require:** The video  $\mathbf{V}$ .

**Ensure:** The key frames  $\mathbf{f} = \{\mathbf{f}^1, \mathbf{f}^2, \dots, \mathbf{f}^K\}$ .

**Step 1** Temporal segmentation.

**1.1** Divide a video  $\mathbf{V}$  into  $\{V_1, V_2, \dots, V_K\}$ , for each segment in  $\{V_1, V_2, \dots, V_K\}$ , we do the following steps.

**Step 2** Convolutional deep feature extraction.

**2.1** Extract deep feature vector  $\mathbf{x}_i^K \leftarrow$  Eq. (3).

**2.2** Map  $\mathbf{x}_i^K$  to feature space  $\mathcal{F}$ .

**Step 3** Density peaks clustering.

**3.1** Calculate  $d_{ij}$  and  $d_{ij} = d_{ji}, i < j, i, j \in I_S$ .

**3.2** Given parameter  $t \in (0, 1]$  to calculate  $d_c$ ,

$$d_c = d_{f(Mt)}, \quad (12)$$

where  $f(Mt)$  denotes the integer after rounding off  $Mt$  and  $M = \frac{1}{2}N(N - 1)$  and  $d_1 \leq d_2 \leq \dots \leq d_M$ .

**3.3** Calculate  $\rho_i \leftarrow$  Eq. (6) or Eq. (8).

**3.4** Calculate  $\delta_i \leftarrow$  Eq. (9).

**3.5** Calculate  $\gamma_i \leftarrow$  Eq. 11.

**return** Index of the key frames  $m_k$  and key frames  $\{\mathbf{f}_{m_k}^K\}_{k=1}^{n_c}$ .

---

framework, which is comprised of six important parts, i.e., block input, input gate, forget gate, cell state, output gate and block output. Let  $\odot$  denote the point-wise multiplication of two vectors, and let  $\sigma(x) = \frac{1}{1+e^{-x}}$  be the sigmoid non-linear activation function which squashes real-valued inputs to a  $[0, 1]$  range, and let  $\phi = \frac{e^x - e^{-x}}{e^x + e^{-x}} = 2\sigma(2x) - 1$  be the hyperbolic tangent nonlinearity activation function, which can also squash its inputs to the range of  $[-1, 1]$ . The LSTM in time step  $t$  given inputs  $x_t$  and  $c_{t-1}$  is defined as follows:

$$g_t = \sigma(W_{xc}x_t + W_{hc}h_{t-1} + b_c), \quad (13)$$

$$i_t = \sigma(W_{xi}x_t + W_{hi}h_{t-1} + b_i), \quad (14)$$

$$f_t = \sigma(W_{xf}x_t + W_{hf}h_{t-1} + b_f), \quad (15)$$

$$c_t = i_t \odot g_t + f_t \odot c_{t-1}, \quad (16)$$

$$o_t = \sigma(W_{xo}x_t + W_{ho}h_{t-1} + b_o), \quad (17)$$

$$h_t = o_t \odot \phi(c_t). \quad (18)$$

In this paper, three layers of LSTM is adopted. The proposed framework of large-scale video classification is composed of two phases, training and testing, and it is summarized in Algorithm 2.

In the training stage, we first obtain the key frames of video  $\mathbf{V}$  via Algorithm 1, then the LSTM model takes over (step 1.1). Next, the LSTM model predicts the video class  $P_f$  at each key frame (step 1.2),

$$P_f = \frac{\exp(W_{hc}h_{t,c} + b_c)}{\sum \exp(W_{hc}h_{t,c'} + b_c)}, \quad (19)$$

**Algorithm 2** The large-scale video classification framework.

**Require:**  $L$  videos for training, corresponds to the labels  $L_{label}$ ;  $T$  testing videos.

**Ensure:** Testing accuracy  $T_{acc}$ .

**Step 1 TRAINING STAGE:**

- 1.1 Extract key frames  $\mathbf{f}$  of  $\mathbf{V} \leftarrow$  Algorithm 1.
- 1.2 The video class  $P_f$  of each key frame  $\leftarrow$  Eq. (19).
- 1.3 The final classification  $R_V \leftarrow$  Eq. (20).
- 1.4 Calculate the weights  $\mathbf{w}$  for different input  $\leftarrow$  Eq. (21) and (22).

**Step 2 TESTING STAGE:**

- 2.1 Extract key frames  $\leftarrow$  Algorithm 1.
- 2.2 The  $P_f$  of each key frame  $\leftarrow$  Eq. (19).
- 2.3 The  $R_V \leftarrow$  Eq. (20).
- 2.4 Computing classification rates of different input.
- 2.5 Combine the weight  $\mathbf{w}$  with each rate.

**return**  $T_{acc}$ .

Table 1. The key characteristics of the datasets used in the experiments.

Dataset	Resolution	Classes	Training	Testing	Total
HMDB51 [27]	$320 \times 240$	51	5,263	1,530	
			5,263	1,530	6,766
			5,263	1,530	
UCF101 [49]	$320 \times 240$	101	9,537	3,783	
			9,586	3,734	13,320
			9,624	3,696	

and we average these predictions for final classification (step 1.3),

$$R_V = \frac{1}{n_c} \sum_{k=1}^{n_c} P_f. \quad (20)$$

Moreover, we propose an approach for the weighted fusion of several inputs networks (i.e., RGB, RGB difference, optical flow and warped flow) that automatically estimates the weight of each input. The weights reflect the relevance of each input for the specific video shot [53]. Note that the proposed weight fusion method is different from the method proposed in [53]. The method in [53] tries to fusion different patch of the same video, while the proposed in this paper tries to combine different modalities of input features. First, we obtain  $t$  classification rates  $\mathbf{r} = \{\mathbf{r}_1, \mathbf{r}_2, \dots, \mathbf{r}_t\}$  for different input networks. We assume that the higher the rate is, the better the feature representation is [53], then the weights can be calculated as follows:

$$t_0 = \frac{\mathbf{r} - \min(\mathbf{r})}{(100 - \min(\mathbf{r}))/10}. \quad (21)$$

The weight of the lowest rate is set to 1, the other weights are set in the direct proportional to 1 based on the ratios to the lowest rate:

$$\begin{aligned} t_1 &= \text{round}(t_0), \\ t_2 &= \frac{t_0 \times (\max(t_1) - 1)}{\max(t_0)} + 1, \\ \mathbf{w} &= \text{round}(t_2), \end{aligned} \quad (22)$$

Table 2. Exploration of different input for the proposed framework on the UCF101 dataset.

Model	Input Type				Weighted			Time (s)
	RGB Image	RGB Difference	Optic Flow	Warped Flow	1/2, 1/2	1/3, 2/3	Ours	
Uniform Sampling (8 frames)	54.36	52.96	58.67	56.39	-	-	55.47	1.63
Uniform Sampling (16 frames)	64.39	61.59	68.36	67.25	-	-	74.29	2.32
Uniform Sampling (32 frames)	68.39	66.59	72.54	72.36	-	-	77.58	3.53
K-means [34]	65.35	63.58	69.69	67.96	-	-	76.67	8.54
S-RNN [47]	73.68	71.56	79.36	78.36	-	-	85.62	7.63
Joint Unsupervised Learning [72]	75.69	73.98	80.49	78.39	-	-	86.39	7.94
Single Frame [9]	65.40	-	53.20	-	-	-	-	-
Single Frame (ave.) [9]	69.00	-	72.20	-	75.71	79.04	-	-
LRCN-fc6 [9]	71.12	-	76.95	-	81.97	82.92	-	-
LRCN-fc7 [9]	70.68	-	69.36	-	-	-	-	-
CNN-TSDPC-LSTM (Ours)	79.63	78.35	-	-	80.63	82.10	-	4.54
CNN-TSDPC-LSTM (Ours)	-	-	84.94	83.63	85.16	86.96	-	4.65
CNN-TSDPC-LSTM (Ours)	79.63	-	84.94	83.63	-	-	93.13	4.87
CNN-TSDPC-LSTM (Ours)	79.63	78.35	84.94	83.63	-	-	91.51	4.96

where  $\mathbf{w}$  is the weight vector of different inputs (step 1.4). During the testing stage, key frames of the testing video are selected in the same way as the training stage (step 2.1). Then we calculate the  $P_f$  and  $R_v$  in the same way as the training stage as well (step 2.2 and 2.3). After that, we compute the classification rates of different inputs and combine the rates with the weights  $\mathbf{w}$  (step 2.4 and 2.5). At the end of the framework, the testing accuracy  $T_{acc}$  of the whole dataset is returned.

## 5 EXPERIMENTS

To evaluate the effectiveness of the proposed method, we conduct experiments with two popular public datasets. More comparisons are shown in Table 1.

### 5.1 Datasets

**HMDB51** dataset<sup>1</sup> contains a total of 6,766 video clips distributed in a large set of 51 action categories collected from various sources, mostly from movies, public datasets and YouTube. Each category contains a minimum of 101 video clips. The videos are taken with the resolution of  $320 \times 240$  with 30 fps.

**UCF101** dataset<sup>2</sup> is a widely-used dataset for action recognition. It comprises of realistic videos collected from YouTube lasting 7 sec. on average. Videos have a spatial resolution of  $320 \times 240$  pixels with 25 fps. UCF101 gives the largest diversity in terms of actions and with the presence of large variations in object appearance, scale and pose, camera motion, viewpoint, cluttered background, illumination conditions.

### 5.2 Setups

For a fair comparison, we set  $t = 0.2$  as in [44]. All the experiments are run at Ubuntu with 2 TITAN Xp GPUs. For one video, the selection process is quite fast with the help of GPUs. We follow existing methods (e.g., [3]) and train our model by using cross-entropy loss.

<sup>1</sup><http://serre-lab.clps.brown.edu/resource/hmdb-a-large-human-motion-database/>

<sup>2</sup><http://crcv.ucf.edu/data/UCF101.php>

Table 3. Mean classification performance of the state-of-the-art approaches on the HMDB51 and UCF101 datasets. Methods on the horizontal line are traditional video classification methods and the approaches under the horizontal line are deep learning methods. \* means the proposed method uses the two-stream I3D as the backbone, and use Kinetics for pre-training.

Method	HMDB51	UCF101
iDT + StackFV [42]	66.8%	-
DT + MHSV [2]	55.9%	83.5%
iDT + FV [63]	57.2%	85.9%
iDT + SFV + STP [62]	60.1%	86.0%
iDT + HSV [41]	61.1%	87.9%
MoFAP [66]	61.7%	88.3%
iDT + MIFS [29]	65.1%	89.1%
VideoDarwin [16]	63.7%	-
MPR [38]	65.5%	-
VGAN [60]	-	52.1%
Deep Networks, Sports 1M pre-training [25]	-	65.2%
C3D (1 net), Sports 1M pre-training [55]	-	82.3%
LRCN (fc6) [9]	-	82.92%
C3D (3 nets), Sports 1M pre-training [55]	-	85.2%
Res3D [56]	54.9%	85.8%
Two Stream [48]	59.4%	88.0%
F <sub>ST</sub> CN (SCI fusion) [51]	59.1%	88.1%
Two Stream + LSTM[73]	-	88.6%
Dynamic Image Networks + IDT [1]	65.2%	89.1%
AdaScan+Two Stream [24]	54.9%	89.4%
C3D (3 nets) + IDT, Sports 1M pre-training [55]	-	90.1%
TDD + FV [65]	63.2%	90.3%
AdaScan+iDT+last fusion [24]	61.0%	91.3%
TDD + iDT [65]	65.9%	91.5%
LTC [58]	64.8%	91.7%
RGB-I3D, miniKinetics pre-training [3]	66.4%	91.8%
Actions Trans [68]	62.0%	92.0%
Convolutional Two Stream [15]	65.4%	92.5%
Hybrid-iDT [8]	70.4%	92.5%
KVMF [75]	63.3%	93.1%
AdaScan+iDT+C3D+last fusion [24]	66.9%	93.2%
TSN (2 modalities, BN-Inception) [67]	68.5%	94.0%
Spatiotemporal Multiplier Network [13]	68.9%	94.2%
TSN (3 modalities, BN-Inception) [67]	69.4%	94.2%
Cool-TSN [43]	69.5%	94.2%
ST-VLMPF(DF) [10]	73.1%	94.3%
Spatiotemporal Pyramid Network [69]	68.9%	94.6%
Spatiotemporal ResNets + IDT [12]	70.3%	94.6%
Flow-I3D, miniKinetics pre-training [3]	72.4%	94.7%
Attention Fusion [33]	-	94.8%
Spatiotemporal Multiplier Network + iDT [13]	72.2%	94.9%
RGB-I3D, Kinetics pre-training [3]	74.8%	95.6%
Optical Flow guided Feature [52]	74.2%	96.0%
Flow-I3D, Kinetics pre-training [3]	77.1%	96.7%
Two-Stream I3D, miniKinetics pre-training [3]	76.3%	96.9%
I3D RGB + DMC-Net (I3D) [46]	77.8%	96.5%
Two-Stream I3D, Kinetics pre-training [3]	80.7%	98.0%
CNN-TSDPC-LSTM (Ours)	75.52%	95.86%
CNN-TSDPC-LSTM* (Ours)	<b>81.44%</b>	<b>98.45%</b>



Fig. 3. A video from the UCF101 dataset, which contains 80 frames. The key frames extracted by the proposed method are in red boxes.

Table 4. Compression Ratio (%) on HMDB51 and UCF101 datasets.

Dataset	#Total Frame	#Avg. Frame	#Total Key Frame	CR(%)
HMDB51	634,552	93.8	108,256	82.94
UCF101	2,485,519	186.6	213,120	91.43

### 5.3 Experimental Results

We present extensive experimental results to demonstrate the necessity and efficiency of the proposed method and framework on large-scale video classification task.

**Comparison of other Extraction Methods.** We first compare different key frames extraction methods on large-scale video classification task. The column “Input Type” of Table 2 shows the performance comparison between our method and the uniform sampling method with different rate (8, 16, 32 frames), k-means [34], S-RNN [47], Joint Unsupervised Learning [72], single frame [9] and LRCN [9] on the UCF101 dataset (split 1). Note that we follow [67] and adopt four different information, i.e., RGB image, RGB difference, optic flow and warped flow as inputs. The results show that our method CNN-TSDPC-LSTM consistently outperforms all the baselines with significant improvements, which validates that there is significant informative motion and spatial information available around key frames. Finally, to better understand and evaluate the proposed key frame extraction method, we show one video example from UCF101 in Figure 3.

**Combination with Weight Strategy.** We then add the proposed weight strategy to our framework to test whether they benefit for this task. As shown in the column “Weighted” of Table 2, the proposed weight method outperforms the

Table 5. Time comparison of different models on UCF101 dataset.

Model	Time
CNN-TSDPC-LSTM (Ours)	1.00
Optical Flow guided Feature [52]	1.13x
Two-Stream I3D [3]	1.35x

Table 6. Computational complexity of different networks.

Network Architecture	GFLOPs
C3D [55]	38.5
Res3D-18 [56]	19.3
ResNet-152 [22]	11.3
ResNet-18 [22]	1.78
PWC-Net [50]	36.15
CNN-TSDPC-LSTM (Ours)	1.45

baseline method LRCN [9] when two inputs (RGB Image and Optic Flow) are employed. Note that “1/2, 1/2” and “1/3, 2/3” are proposed in [9] and are two different weight settings which represent the fixed weights of two different inputs. Besides, when we adopt three inputs, i.e., RGB image, optic flow and warped flow, we achieve the best performance compared with other baselines. However, we observe that introduce RGB difference will degrade the performance, which is also observed in TSN [67].

**Comparison with State-of-the-Art Methods.** We assemble these three inputs and all the techniques described as our final video classification method, and test it on both HMDB51 and UCF101 datasets. For both HMDB51 and UCF101 datasets, we compare the proposed framework i.e., CNN-TSDPC-LSTM-Fusion, with the state-of-the-art traditional approaches, e.g., iDT + HSV [41] and MoFAP [66]. We also compare the proposed method with deep learning representation methods such as LRCN [9], KVMF [75] and TSN [67]. The results are summarized in Table 3, our method achieves competitive classification accuracy compared with these methods. Note that the classification performance of the proposed framework is worse than several of baselines such as Two-Stream I3D [3]. Carreira and Zisserman [3] achieve the best performance after pre-training on extra data, i.e., Kinetics. However, the proposed method is more efficient and has a higher compression ratio which is defined as the relative amount of savings provided by the summary representation. The definition of the compression ratio is,  $CR(V) = 1 - \frac{n_c}{N}$ , where  $n_c$  and  $N$  are the number of key frames and the number of frames in the original video  $V$  respectively. The results are shown in Table 4. Generally, a high compression ratio means for a compact video summary and also means less video processing time. Finally, to further prove the effectiveness of our proposed method, we use the two-stream I3D as our backbone, and use Kinetics for pre-training. As can be seen from Table 3, this model achieves state-of-the-art results on both datasets.

**Efficiency Comparison.** We also measure the average classification time on UCF101 dataset. The column “Time” of Table 2 lists the average time of different sampling approaches. The results showing that we can obtain high classification accuracy while keeping the complexity low compared with the state-of-the-art key frame extraction methods such as S-RNN [47] and Joint Unsupervised Learning [72]. Consequently, the proposed method is time efficient both on-line and off-line, and can be readily adopted in real-world applications. Moreover, as we expected we observe that more inputs consumer more times. We also provide time comparison with the state of the art methods on UCF101 dataset.

Results are shown in Table 5, we can see that the proposed method is faster than Optical Flow guided Feature [52] and Two-Stream I3D [3]. In Table 6, we also provide the GFLOPs results compared with other network architectures for video analysis, including ResNet-18 [22], ResNet-152 [22], C3D [55], and Res3D [56]. We observe that the complexity of the proposed method is smaller compared to that of other architectures, which makes it run much faster.

## 6 CONCLUSION

We present an unsupervised key frame extraction method, i.e., TSDPC, for video key frame extraction, which can greatly reduce the redundant information of the original video while preserve the temporal information through selecting the number of key frames automatically. In addition, a framework CNN-TSDPC-LSTM aimed at large-scale video classification which consists of CNN, TSDPC and LSTM is proposed. Moreover, a fusion strategy of different input networks is presented to boost the accuracy of video classification. Experimental results on a variety of public datasets demonstrate that (i) our framework is capable of summarizing video efficiently regardless of the visual content of videos. (ii) our framework is with high efficiency while the mean classification accuracy is comparable with other state-of-the-art methods. Note that the proposed method is generic, which thus can be beneficial to other video processing tasks.

## ACKNOWLEDGMENTS

This work is supported by the PRIN project PREVUE (Prot. 2017N2RK7K) and by the EU H2020 project AI4Media under Grant 951911.

## REFERENCES

- [1] Hakan Bilen, Basura Fernando, Efstratios Gavves, Andrea Vedaldi, and Stephen Gould. 2016. Dynamic image networks for action recognition. In *CVPR*.
- [2] Zhuowei Cai, Limin Wang, Xiaojiang Peng, and Yu Qiao. 2014. Multi-view super vector for action recognition. In *CVPR*.
- [3] Joao Carreira and Andrew Zisserman. 2017. Quo Vadis, Action Recognition? A New Model and the Kinetics Dataset. In *CVPR*.
- [4] Zuzana Černáková, Ioannis Pitas, and Christophoros Nikou. 2006. Information theory-based shot cut/fade detection and video summarization. *IEEE TCSVT* 16, 1 (2006), 82–91.
- [5] Vasileios Choutas, Philippe Weinzaepfel, Jérôme Revaud, and Cordelia Schmid. 2018. Potion: Pose motion representation for action recognition. In *CVPR*.
- [6] Yang Cong, Junsong Yuan, and Jiebo Luo. 2012. Towards scalable summarization of consumer videos via sparse dictionary selection. *IEEE TMM* 14, 1 (2012), 66–75.
- [7] Sandra Eliza Fontes De Avila, Ana Paula Brandão Lopes, Antonio da Luz, and Arnaldo de Albuquerque Araújo. 2011. VSUMM: A mechanism designed to produce static video summaries and a novel evaluation method. *Elsevier PRL* 32, 1 (2011), 56–68.
- [8] César Roberto de Souza, Adrien Gaidon, Eleonora Vig, and Antonio Manuel López. 2016. Sympathy for the details: Dense trajectories and hybrid classification architectures for action recognition. In *ECCV*.
- [9] Jeffrey Donahue, Lisa Anne Hendricks, Sergio Guadarrama, Marcus Rohrbach, Subhashini Venugopalan, Kate Saenko, and Trevor Darrell. 2015. Long-term recurrent convolutional networks for visual recognition and description. In *CVPR*.
- [10] Ionut Cosmin Duta, Bogdan Ionescu, Kiyoharu Aizawa, and Nicu Sebe. 2017. Spatio-Temporal Vector of Locally Max Pooled Features for Action Recognition in Videos. In *CVPR*.
- [11] Naveed Ejaz, Tayyab Bin Tariq, and Sung Wook Baik. 2012. Adaptive key frame extraction for video summarization using an aggregation mechanism. *Elsevier JVCIP* 23, 7 (2012), 1031–1040.
- [12] Christoph Feichtenhofer, Axel Pinz, and Richard Wildes. 2016. Spatiotemporal residual networks for video action recognition. In *NIPS*.
- [13] Christoph Feichtenhofer, Axel Pinz, and Richard P Wildes. 2017. Spatiotemporal multiplier networks for video action recognition. In *CVPR*.
- [14] Christoph Feichtenhofer, Axel Pinz, Richard P Wildes, and Andrew Zisserman. 2018. What have we learned from deep representations for action recognition?. In *CVPR*.
- [15] Christoph Feichtenhofer, Axel Pinz, and Andrew Zisserman. 2016. Convolutional two-stream network fusion for video action recognition. In *CVPR*.
- [16] Basura Fernando, Efstratios Gavves, Jose M Oramas, Amir Ghodrati, and Tinne Tuytelaars. 2015. Modeling video evolution for action recognition. In *CVPR*.
- [17] Adrien Gaidon, Zaid Harchaoui, and Cordelia Schmid. 2013. Temporal localization of actions with actoms. *IEEE TPAMI* 35, 11 (2013), 2782–2795.

- [18] Ruohan Gao, Bo Xiong, and Kristen Grauman. 2018. Im2Flow: Motion Hallucination from Static Images for Action Recognition. In *CVPR*.
- [19] Hana Gharbi, Sahbi Bahroun, Mohamed Massaoudi, and Ezzeddine Zagrouba. 2017. Key frames extraction using graph modularity clustering for efficient video summarization. In *ICASSP*.
- [20] Genliang Guan, Zhiyong Wang, Shiyang Lu, Jeremiah Da Deng, and David Dagan Feng. 2013. Keypoint-based keyframe selection. *IEEE TCSVT* 23, 4 (2013), 729–734.
- [21] Kensho Hara, Hirokatsu Kataoka, and Yutaka Satoh. 2018. Can spatiotemporal 3d cnns retrace the history of 2d cnns and imagenet?. In *CVPR*.
- [22] Kaiming He, Xiangyu Zhang, Shaoqing Ren, and Jian Sun. 2016. Deep residual learning for image recognition. In *CVPR*.
- [23] Shuiwang Ji, Wei Xu, Ming Yang, and Kai Yu. 2013. 3D convolutional neural networks for human action recognition. *IEEE TPAMI* 35, 1 (2013), 221–231.
- [24] Amlan Kar, Nishant Rai, Karan Sikka, and Gaurav Sharma. 2017. AdaScan: Adaptive Scan Pooling in Deep Convolutional Neural Networks for Human Action Recognition in Videos. In *CVPR*.
- [25] Andrej Karpathy, George Toderici, Sanketh Shetty, Thomas Leung, Rahul Sukthankar, and Li Fei-Fei. 2014. Large-scale video classification with convolutional neural networks. In *CVPR*.
- [26] Sanjay K Kuanar, Rameswar Panda, and Ananda S Chowdhury. 2013. Video key frame extraction through dynamic Delaunay clustering with a structural constraint. *Elsevier JVCIP* 24, 7 (2013), 1212–1227.
- [27] H. Kuehne, H. Jhuang, E. Garrote, T. Poggio, and T. Serre. 2011. HMDB: a large video database for human motion recognition. In *ICCV*.
- [28] Sourabh Kulhare, Shagan Sah, Suhas Pillai, and Raymond Ptucha. 2016. Key frame extraction for salient activity recognition. In *ICPR*.
- [29] Zhengzhong Lan, Ming Lin, Xuanchong Li, Alex G Hauptmann, and Bhiksha Raj. 2015. Beyond gaussian pyramid: Multi-skip feature stacking for action recognition. In *CVPR*.
- [30] Ivan Laptev, Marcin Marszalek, Cordelia Schmid, and Benjamin Rozenfeld. 2008. Learning realistic human actions from movies. In *CVPR*.
- [31] Hong Liu, Hao Tang, Wei Xiao, ZiYi Guo, Lu Tian, and Yuan Gao. 2016. Sequential Bag-of-Words model for human action classification. *CAAI Transactions on Intelligence Technology* 1, 2 (2016), 125–136.
- [32] Hong Liu, Lu Tian, Mengyuan Liu, and Hao Tang. 2015. Sdm-bsm: A fusing depth scheme for human action recognition. In *ICIP*.
- [33] Xiang Long, Chuang Gan, Gerard de Melo, Xiao Liu, Yandong Li, Fu Li, and Shilei Wen. 2018. Multimodal keyless attention fusion for video classification. In *AAAI*.
- [34] James MacQueen et al. 1967. Some methods for classification and analysis of multivariate observations. In *Proceedings of the fifth Berkeley symposium on mathematical statistics and probability*.
- [35] Shaohui Mei, Genliang Guan, Zhiyong Wang, Mingyi He, Xian-Sheng Hua, and David Dagan Feng. 2014. L 2, 0 constrained sparse dictionary selection for video summarization. In *ICME*.
- [36] Shaohui Mei, Genliang Guan, Zhiyong Wang, Shuai Wan, Mingyi He, and David Dagan Feng. 2015. Video summarization via minimum sparse reconstruction. *Elsevier PR* 48, 2 (2015), 522–533.
- [37] Jingjing Meng, Hongxing Wang, Junsong Yuan, and Yap-Peng Tan. 2016. From keyframes to key objects: Video summarization by representative object proposal selection. In *CVPR*.
- [38] Bingbing Ni, Pierre Moulin, Xiaokang Yang, and Shuicheng Yan. 2015. Motion part regularization: Improving action recognition via trajectory selection. In *CVPR*.
- [39] Costas Panagiotakis, Anastasios Doulamis, and Georgios Tziritas. 2009. Equivalent key frames selection based on iso-content principles. *IEEE TCSVT* 19, 3 (2009), 447–451.
- [40] Rameswar Panda, Sanjay K Kuanar, and Ananda S Chowdhury. 2014. Scalable video summarization using skeleton graph and random walk. In *ICPR*.
- [41] Xiaojiang Peng, Limin Wang, Xingxing Wang, and Yu Qiao. 2016. Bag of visual words and fusion methods for action recognition: Comprehensive study and good practice. *Elsevier CVIU* 150 (2016), 109–125.
- [42] Xiaojiang Peng, Changqing Zou, Yu Qiao, and Qiang Peng. 2014. Action recognition with stacked fisher vectors. In *ECCV*. 581–595.
- [43] Cesar Roberto de Souza, Adrien Gaidon, Yohann Cabon, and Antonio Manuel Lopez. 2017. Procedural Generation of Videos to Train Deep Action Recognition Networks. In *CVPR*.
- [44] Alex Rodriguez and Alessandro Laio. 2014. Clustering by Fast Search and Find of Density Peaks. *Science* 344, 6191 (2014), 1492–1496.
- [45] Olga Russakovsky, Jia Deng, Hao Su, Jonathan Krause, Sanjeev Satheesh, Sean Ma, Zhiheng Huang, Andrej Karpathy, Aditya Khosla, Michael Bernstein, et al. 2015. Imagenet Large Scale Visual Recognition Challenge. *Springer IJCV* 115, 3 (2015), 211–252.
- [46] Zheng Shou, Xudong Lin, Yannis Kalantidis, Laura Sevilla-Lara, Marcus Rohrbach, Shih-Fu Chang, and Zhicheng Yan. 2019. Dmc-net: Generating discriminative motion cues for fast compressed video action recognition. In *CVPR*.
- [47] Gunnar A Sigurdsson, Xinlei Chen, and Abhinav Gupta. 2016. Learning visual storylines with skipping recurrent neural networks. In *ECCV*.
- [48] Karen Simonyan and Andrew Zisserman. 2014. Two-stream convolutional networks for action recognition in videos. In *NIPS*.
- [49] Khurram Soomro, Amir Roshan Zamir, and Mubarak Shah. 2012. UCF101: A dataset of 101 human actions classes from videos in the wild. *arXiv preprint arXiv:1212.0402* (2012).
- [50] Deqing Sun, Xiaodong Yang, Ming-Yu Liu, and Jan Kautz. 2018. Pwc-net: Cnns for optical flow using pyramid, warping, and cost volume. In *CVPR*.
- [51] Lin Sun, Kui Jia, Dit-Yan Yeung, and Bertram E Shi. 2015. Human action recognition using factorized spatio-temporal convolutional networks. In *ICCV*.

- [52] Shuyang Sun, Zhanghui Kuang, Lu Sheng, Wanli Ouyang, and Wei Zhang. 2018. Optical flow guided feature: a fast and robust motion representation for video action recognition. In *CVPR*.
- [53] Hao Tang, Hong Liu, and Wei Xiao. 2015. Gender Classification Using Pyramid Segmentation for Unconstrained Back-facing Video Sequences. In *ACM MM*.
- [54] Hao Tang, Hong Liu, Wei Xiao, and Nicu Sebe. 2019. Fast and robust dynamic hand gesture recognition via key frames extraction and feature fusion. *Elsevier Neurocomputing* 331 (2019), 424–433.
- [55] Du Tran, Lubomir Bourdev, Rob Fergus, Lorenzo Torresani, and Manohar Paluri. 2015. Learning spatiotemporal features with 3d convolutional networks. In *ICCV*.
- [56] Du Tran, Jamie Ray, Zheng Shou, Shih-Fu Chang, and Manohar Paluri. 2017. Convnet architecture search for spatiotemporal feature learning. *arXiv preprint arXiv:1708.05038* (2017).
- [57] Du Tran, Heng Wang, Lorenzo Torresani, Jamie Ray, Yann LeCun, and Manohar Paluri. 2018. A Closer Look at Spatiotemporal Convolutions for Action Recognition. In *CVPR*.
- [58] GÜl Varol, Ivan Laptev, and Cordelia Schmid. 2017. Long-term temporal convolutions for action recognition. *IEEE TPAMI* 40, 6 (2017), 1510–1517.
- [59] Ricardo Vázquez-MartíN and Antonio Bandera. 2013. Spatio-temporal feature-based keyframe detection from video shots using spectral clustering. *Elsevier PRL* 34, 7 (2013), 770–779.
- [60] Carl Vondrick, Hamed Pirsiavash, and Antonio Torralba. 2016. Generating videos with scene dynamics. In *NIPS*.
- [61] Hongxing Wang, Yoshinobu Kawahara, Chaoqun Weng, and Junsong Yuan. 2017. Representative selection with structured sparsity. *Elsevier PR* 63 (2017), 268–278.
- [62] Heng Wang, Dan Oneata, Jakob Verbeek, and Cordelia Schmid. 2016. A robust and efficient video representation for action recognition. *Springer IJCV* 119, 3 (2016), 219–238.
- [63] Heng Wang and Cordelia Schmid. 2013. Action recognition with improved trajectories. In *ICCV*.
- [64] Limin Wang, Yu Qiao, and Xiaou Tang. 2014. Latent hierarchical model of temporal structure for complex activity classification. *IEEE TIP* 23, 2 (2014), 810–822.
- [65] Limin Wang, Yu Qiao, and Xiaou Tang. 2015. Action recognition with trajectory-pooled deep-convolutional descriptors. In *CVPR*.
- [66] Limin Wang, Yu Qiao, and Xiaou Tang. 2016. MoFAP: A multi-level representation for action recognition. *Springer IJCV* 119, 3 (2016), 254–271.
- [67] Limin Wang, Yuanjun Xiong, Zhe Wang, Yu Qiao, Dahua Lin, Xiaou Tang, and Luc Van Gool. 2016. Temporal segment networks: Towards good practices for deep action recognition. In *ECCV*.
- [68] Xiaolong Wang, Ali Farhadi, and Abhinav Gupta. 2016. Actions<sup>~</sup> transformations. In *CVPR*.
- [69] Yunbo Wang, Mingsheng Long, Jianmin Wang, and Philip S Yu. 2017. Spatiotemporal Pyramid Network for Video Action Recognition. In *CVPR*.
- [70] Yali Wang, Lei Zhou, and Yu Qiao. 2018. Temporal Hallucinating for Action Recognition with Few Still Images. In *CVPR*.
- [71] Chao-Yuan Wu, Manzil Zaheer, Hexiang Hu, R Manmatha, Alexander J Smola, and Philipp Krähenbühl. 2018. Compressed video action recognition. In *CVPR*.
- [72] Jianwei Yang, Devi Parikh, and Dhruv Batra. 2016. Joint unsupervised learning of deep representations and image clusters. In *CVPR*.
- [73] Joe Yue-Hei Ng, Matthew Hausknecht, Sudheendra Vijayanarasimhan, Oriol Vinyals, Rajat Monga, and George Toderici. 2015. Beyond short snippets: Deep networks for video classification. In *CVPR*.
- [74] Yizhou Zhou, Xiaoyan Sun, Zheng-Jun Zha, and Wenjun Zeng. 2018. MiCT: Mixed 3D/2D Convolutional Tube for Human Action Recognition. In *CVPR*.
- [75] Wangjiang Zhu, Jie Hu, Gang Sun, Xudong Cao, and Yu Qiao. 2016. A key volume mining deep framework for action recognition. In *CVPR*.
- [76] Yi Zhu, Yang Long, Yu Guan, Shawn Newsam, and Ling Shao. 2018. Towards Universal Representation for Unseen Action Recognition. In *CVPR*.
- [77] Yuetong Zhuang, Yong Rui, Thomas S Huang, and Sharad Mehrotra. 1998. Adaptive key frame extraction using unsupervised clustering. In *ICIP*.